The United Nations University

GEOTHERMAL TRAINING PROGRAMME
Orkustofnun, Grensásvegur 9,
IS-108 Reykjavík, Iceland

Reports 1998
Number 7

HYDROGEN SULPHIDE DISPERSION MODELLING FOR THE SVARTSENGI GEOTHERMAL POWER PLANT, SW-ICELAND

Pius W. Kollikho
The Kenya Electricity Generating Company,
Olkaria Geothermal Project,
P.O. Box 785, Naivasha,
KENYA

ABSTRACT

Results of H_2S predictions for 1, 3, 8 and 24 hour, monthly and annual concentrations for emissions from Svartsengi power plant, using the Industrial Source Complex Model (ISC3View) and Air Force Toxic Chemical Dispersion Model (AFTOX) are presented. In all cases higher concentrations are predicted towards the northeast and southwest site of the power plant, and concentrations decline with increasing distance. Annual predictions are in good agreement with the 24 hour measurements averaged over the same duration. Short term predictions seemed to overestimate measured concentrations. The ISC3View model predicts a maximum 1 hour average of 1720 $\mu g/m^3$, 280 $\mu g/m^3$ for 24 hours and annual average of 27 $\mu g/m^3$. The measurements done over a short averaging time (1 minute) indicate lower maximum concentrations (265 $\mu g/m^3$) than model results. The H_2S pattern around Svartsengi follows the annual wind pattern with high concentrations in the regions characterised by high frequency of wind towards that direction.

1. INTRODUCTION

Gaseous modelling studies have been widely used in environmental studies in many parts of the world. Gaussian puff models use an equation to describe the dispersion of a puff with time. In these studies, the meteorological conditions and emission scenarios are used to predict the expected concentrations or wet/dry deposition rates. The ISC3 have been applied extensively throughout the world (US Environmental Protection Agency, 1995). Modelling results are used to assess whether pollution abatement technology, including stack height selection, adequately satisfy occupational exposure levels (OELs) and public exposure levels, i.e. air quality standards (AQSs).

Modelling studies have also been used in studying the transport of plumes from cooling towers (Salerno and Clerici, 1995). In all cases, the importance of meteorological conditions and topography, have been emphasised. As geothermal development all over the world continues to grow, the environmental impact assessment (EIA) has become an important part of the implementation process. This has been partly due to the mandatory regulations, acts and statutes of most countries, or requirements by funding agencies

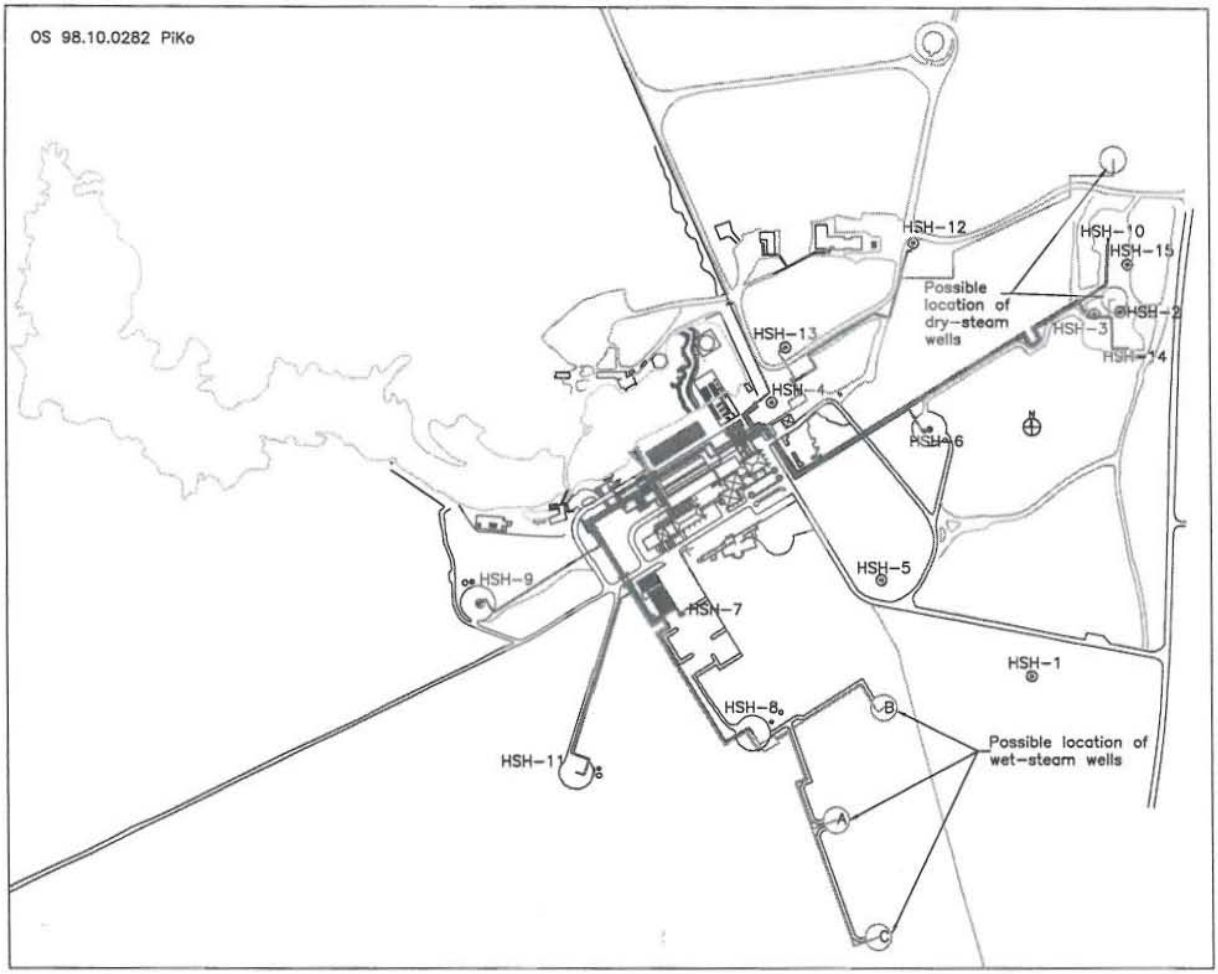

FIGURE 1: Svartsengi power plant settings, including the Blue Lagoon

like the World Bank and the European Bank. In some cases, administering agencies have asked for EIA.

This requirement has often been enhanced by the fact that many geothermal projects are located in remote areas, or national parks, like the Olkaria power project in Naivasha, Kenya. The development of the Olkaria North East power project was preceded by an environmental impact assessment (Sinclair Knight and ESA Pty Ltd., 1994).

The main objective of the present study, was to

1) Predict H_2S concentrations from emissions at the Svartsengi geothermal power plant in August - December 1994, based on the meteorological and emission scenarios then;
2) Compare the predicted results to the actual measurements made.

Initially, the study was intended also to cover both the Nesjavellir and Krafla areas, but due to insufficient meteorological data, only the Svartsengi area was considered.

Project description. The site under study, Svartsengi, is shown in Figure 1. The grid network was 1.375 km by 1 km, thus enclosing the power plant and the surroundings, including the Blue Lagoon. There are 16 x 11 receptor points, with each grid measuring 100 x 100 m. The origin was set at -718500, 382200.

2. MODEL DESCRIPTION

This chapter deals with a brief description of the AFTOX and ISC3View models and the mathematical formulations involved in both.

2.1 AFTOX and ISC3View models

Both the AFTOX and ISC3View models are Gaussian puff/plume dispersion models designed for two emission categories; continuous (steady-state) or instantaneous (transient). In steady-state releases, source characteristics do not vary with time (i.e. emission rate is constant), and the release duration is long compared to advection (travel) time. For transient release, the source characteristics do not vary with time but the duration of the release from the source is limited.

In the AFTOX model, a Gaussian puff model uses an equation to describe the dispersion of a puff with time. It assumes that the material is conserved during transport and diffusion, that is, there is no decay or deposition. The distribution of the concentration within the puff is assumed to be Gaussian. The ISC3View model on the other hand, takes care of the deposition and decay.

2.2 The Gaussian diffusion equation

The Gaussian diffusion equation can be written as follows:

$$G(x,y,z,t-t') = \frac{Q(t')}{2\pi^{3/2}(\sigma_x\sigma_y\sigma_z)}\exp[-\frac{1}{2}(\frac{(x-u(t-t')}{\sigma_x})^2]\exp[-\frac{1}{2}(\frac{y}{\sigma_y})^2]\exp[-\frac{1}{2}(\frac{z-H}{\sigma_z})^2]+\exp[-\frac{1}{2}(\frac{z+H}{\sigma_z})] \quad (1)$$

where G = Concentration in the puff at a given point (x,y,z) and time $(t-t')$;
Q = Total mass in the puff;
σ_x, σ_y, σ_z, = Diffusion parameters, which are the standard deviation of the material concentration in the x, y, and z directions; it is assumed that $\sigma_x = \sigma_y$, thus producing a circular horizontal puff cross-section.
t = Total elapsed time since the spill;
t' = Time of emission of the puff, thus, $(t-t')$ is the travel time or the elapsed time since puff emission;
u = Wind speed at 10 m elevation; and
H = Height of the source.

When there is an inversion, Equation 1 can be re-written by adding of the following two expressions to the last two terms:

$$\sum \exp[-\frac{1}{2}(\frac{z-H-2NL}{\sigma_z})^2]+\exp[-\frac{1}{2}(\frac{z+H-2NL}{\sigma_z})^2]+\exp[-\frac{1}{2}(\frac{z-H+2NL}{\sigma_z})^2]+\exp[-\frac{1}{2}(\frac{z+H+2NL}{\sigma_z})^2] \quad (2)$$

where L = Mixing layer height; and
N = Number of iterations.

The computer program considers the series converged when the above expression has a value less than 0.01 for given N. If there is no inversion, the expression is ignored in the program. When the series requires a large number of iterations to converge (>200), the program assumes a uniformly distributed

plume between the earth's surface and the inversion height. If this is the case, then the concentration at a given point and time in the puff is described by the following equation:

$$G(x,y,z,t-t') = \frac{Q(t')}{2\pi\sigma_x\sigma_y L} \times \exp -\frac{1}{2}[\frac{x-u(t-t')}{\sigma_x}]^2 \times [-\frac{1}{2}(\frac{y}{\sigma_y})^2] \quad (3)$$

The concentration at a point in space depends on; the number of nearby puffs, their size, and the amount of material in each puff. Summing up all emission times to get the effect of all these puffs will result in:

$$G(x,y,z,t) = \sum_{t=0}^{\infty} G(x,y,z,t-t') \quad (4)$$

For an instantaneous gas release, there is only one emission time and puff. Therefore, summation is not necessary. For continuous spill, the summation is performed over puffs whose centres are located within four standard deviations of the spill upwind and downwind from the location of interest. It is assumed that concentrations from puffs further than four standard deviations contribute little to the concentration at the specified location.

Under steady-state, non-inversion conditions, keeping track of the individual puff is not necessary. A simple Gaussian plume will be used instead of Equation 1. The equation has the form

$$C = \frac{Q}{2\pi\sigma_x\sigma_y u} \times \exp[-\frac{1}{2}(\frac{y}{\sigma_y})^2] \times \exp[-\frac{1}{2}(\frac{z-H}{\sigma_z})^2] + \exp[-\frac{1}{2}(\frac{z+H}{\sigma_z})^2] \quad (5)$$

2.2.1 The Gaussian equation for the ISC3View model

The ISC3View model for stacks uses the steady-state Gaussian plume equation for a continuous elevated source. For each source and each hour, the origin of the source's coordinate system is placed at ground surface at the base of the stack. The x axis is positive in the downwind direction, the axis is crosswind (normal) to the y axis and the z axis extends vertically. The fixed receptor locations are converted to each source's coordinate system for each hourly concentration calculation. The hourly concentrations calculated for each source at each receptor are summed up to obtain the total concentration produced at each receptor by the combined source emissions.

For a steady-state Gaussian plume, the hourly concentration at downwind distance x (m) and crosswind distance y (m) is given by:

$$C = \frac{QKVD}{2\pi u_s\sigma_y\sigma_z} \exp[-\frac{1}{2}(\frac{y}{\sigma_y})^2] \quad (6)$$

where Q = Pollutant emission rate (mass per unit time);
K = Scaling coefficient to convert calculated concentrations to desired units (default value for Q of 1 x 10^6 g/s and concentration in $\mu g/m^3$);
V = Vertical term;
D = Decay term;
σ_x σ_y = Standard deviation of lateral and vertical concentration distribution (m);
u_s = Wind speed at release height (m/s).

Average removal rates of hydrogen sulphide have been estimated by Cox and Sheppard (1980) and Cox

and Sandalls (1974). Using an average reaction rate $5x10^{-12}$ cm^3/s and an average hydroxyl concentration of $3x10^6$ molecules/m^3, an average removal rate of hydrogen sulphide was estimated to be approximately 5 % / hour. This will give an exponential decay rate of $1.425x10^{-5}s^{-1}$ when used in the ISC3 View model.

Model runs with and without the decay showed very little difference over the grid for the Olkaria study (Sinclair Knight and ESA Pty Ltd, 1994). In the present study, a similar removal rate of 5% / hour was used.

2.2.2 Atmospheric stability

Together with the distance from source, the atmospheric stability affects the dispersion parameters (σ_x, σ_y). It is often defined by the Pasquill stability categories, which range from category A for a very unstable atmosphere to F for a very stable atmosphere. In AFTOX, a continuous stability parameter ranging from 0.5 to 6 is used in place of the discrete stability categories. The relationship between the Pasquill stability category and the continuous parameter is shown in Table1.

TABLE 1: The relationship between the Pasquill stability categories, SC, and the continuous parameter, SP, used in AFTOX

SC	A	B	C	D	E	F
SP	0.5-1	1-2	2-3	3-4	4-5	5-6

To define the stability parameter, AFTOX employs one of two methods, using wind speed and solar insolation, or using the standard deviation of the wind direction to define the stability parameter. In the former case, Golder's nomogram (Golder, 1972) is used to determine stability, where the Monin-Obukhov length (L) and surface roughness are related to the Pasquill stability categories. Since L is a function of friction velocity, u_* and sensible heat flux H, these two parameters must also be calculated. In the latter case, stability is obtained by calculation using the Modified Sigma Theta (MST) approach (Mitchell, 1982).

2.2.3 Determination of u_* and L

To determine u_* m/s and L, the iterative procedure used has been summarised by Ragland and Dennis (1975), for neutral, unstable, and stable conditions.

Neutral:

$$\frac{ku}{u_*} = \ln\frac{Z}{Z_o} \tag{7}$$

Unstable:

$$\frac{ku}{u_*} = 2(\tan^{-1}x - \tan^{-1}x_o) + \ln\frac{x+1}{x_o+1} - \ln\frac{x+1}{x_o+1} \tag{8}$$

where $x = (1 - 15Z/L)^{1/4}$ and $x_o = (1 - 15Z_o/L)^{1/4}$.

Stable:

$$\frac{ku}{u_*} = \ln\frac{Z}{Z_o} + 5.2\alpha \tag{9}$$

where u = Measured wind speed;
u_* = Friction velocity;
k = Von Karman constant,
Z = Anemometer height;
Z_o = Roughness length at the wind measurement site,
L = Monin-Obukhov length (m), and;
α = Z/L when $Z < L$ and $\alpha = 1$ when $Z > L$.

The Monin-Obukhov length L is a measure of atmospheric stability and is defined as

$$L = -\frac{\rho C_p T u_*^3}{kgH} \tag{10}$$

where ρ = Ambient air density;
C_p = Specific heat of air;
T = Air temperature;
k = Von Karman constant;
g = Acceleration due to gravity (ms^{-2}), and;
H = Sensible heat flux (W/m^2).

Equation 10 can be rewritten as

$$L = -\frac{pu_*^3}{0.0112H} \tag{11}$$

where p = Atmospheric pressure (mbar).

To start the iteration, an estimate of u_* is required. This is calculated from Equation 11

$$u_* = \frac{1}{12}\left(u + \frac{0.8H}{H+1000}\right) \tag{12}$$

were wind speed, u, at 10 m is estimated from the measured wind, u_z using the power law;

$$u = u_z\left(\frac{10}{z}\right)^{0.2} \tag{13}$$

The iteration continues until successive values of u_*/u differ by less than 0.001. L is then calculated from this value of u_*. Once u_* is derived, the wind speed at 10 m is determined and used in the Gaussian puff equation (Equation 1)/or the plume equation (Equation 5).

2.2.4 Calculating the sensible heat flux

Sensible heat flux, H, is needed for calculating the Monin-Obukhov length, L, and for determining the appropriate wind profile equation. A positive heat flux greater than 1 W/m^2 is unstable (Equation 8), while a negative heat flux less than -1 W/m^2 is stable (Equation 9). A heat flux between 1 and -1 W/m^2 is neutral (Equation 10). The sensible heat flux is also used to determine the initial estimates of u_*. Holtslag and Van Ulden (1983) describe a method for determining it for daytime conditions.

Under clear skies, the incoming solar radiation at ground level, SR, a function of the solar elevation angle, ϕ, can be determined from the following empirical formula:

$$SR_o = a_1 \sin\phi + a_2 \tag{14}$$

The turbidity coefficients, a_1 and a_2, describe the average atmospheric attenuation by water vapour and dust for a gives site. These coefficients will vary from one location to another and from one period to another because of the variation in the turbidity of the atmosphere. In this model, a_1 = 990 W/m^2 and a_2 = -30 W/m^2 were used since they represent a reasonable average of coefficients determined at various locations.

The effect of the clouds is reduction of incoming solar radiation. Kasten and Czeplak (1980) have proposed the following:

$$SR = SR_o(1 + b_1 N^{b_2}) \tag{15}$$

where N = Fraction of sky covered with clouds,
b_1 , b_2 = Empirical coefficients.

From ten years of observation at Hamburg, they obtained b_1 = -0.75 and b_2 = 3.4 on average. This means that the solar radiation reaching the ground under overcast conditions is 25 percent of that reaching the ground under clear skies. They also showed that the transmittances, TR, of cirrus, altus, cumulus, stratus, and nimbostratus are 0.61, 0.27, 0.25, 0.18, and 0.16, respectively. To take into account the type of cloud, Equation 15 has been modified to read

$$SR = SR_o(1 - (1 - TR) b_1 N^{b_2}) \tag{16}$$

In the model, three cloud groups for high, medium and low clouds are used as shown in Table 2.

TABLE 2: Transmittances for high, medium and low clouds

High	Ci, Cc, Cs	0.61
Medium	Ac, As, Sc, Cu	0.26
Low	St, Ns, Fog	0.17

The net radiation is determined from the following equation:

$$Q = \frac{(1 - r)SR + C_1 T^6 - \sigma T^4 + C_2 N}{1 + C_3} \tag{17}$$

where r = Albedo of surface, equal to 0.25, except when there is snow cover, when set at 0.75;
T = Air temperature (K);
σ = Stefan-Boltzmann constant, equal to 5.67 x 10^{-8} W/m^2 K^4;
C_1 ,C_2 = Empirical constants, equal to 5.31 x 10^{-13} W/m^2 K^{-6} and 60 W/m^2, respectively;
C_3 = Surface heating coefficients that varies from 0.12 for a wet surface to 0.38 for dry, bare soil. In the model, C_3 is equal to 0.12 for a wet surface and 0.25 for a dry surface.

The surface energy budget relates the net radiation, Q, to the various heat fluxes at the earth's surface.

$$H+\lambda E+G = Q \tag{18}$$

where H = Sensible heat flux;
λE = Latent heat flux, and;
G = Soil heat flux which is set to equal 0.1 Q. If the surface is covered with snow, $G = 0$ to reflect poor conductivity of snow.

A simplified parameterization for the sensible heat flux, H, and latent heat flux, E is presented by DeBruin and Holtslag (1982)

$$H = \frac{1-\alpha+\gamma/s}{1+\gamma/s}(Q-G)-\beta'\gamma \tag{19}$$

$$E = \frac{\alpha}{1+\gamma/s}(Q-G)+\beta'\gamma \tag{20}$$

where
s = q_s/T, and q_s is the saturation specific humidity;
γ = C_p/λ where C_p is the specific heat of air at constant pressure and λ the latent heat of vaporization, and;
α and β'= Empirical parameters.

A regression line has been fitted into the data by Holtslag and Van Ulden (1983) as shown by Equation 21,

$$\gamma/s = 119.56-0.7843T+1.2887x10^{-3}T^2 \tag{21}$$

where T is the temperature, (K).

The surface moisture parameter is set at 1.0 for wet conditions and 0.45 for dry conditions. The parameter β' is set at 20 W/m^2.

For nighttime, the sensible heat flux, H, (Wm^2) is related to the total cloud cover, N, as shown by Smith (1972).

$$H = -40(1-N) \tag{22}$$

2.2.5 Calculating the solar elevation angle

The solar elevation angle for a given time and location may be calculated by the following method as described by Woolf (1980).

$$\sin\phi = \sin LA \sin D + \cos LA \cos D \cos H \tag{23}$$

where LA = Station latitude;
D = Solar declination angle, and;
H = Solar hour angle.

Solar declination angle is a sinusoidal function of time with maximum and minimum angles occurring during summer and winter, respectively. There is a slight asymmetry, due to the ellipticity of the earth's orbit, which is accounted for in the following expression for calculating declination:

$$\sin D = \sin 23.4438 \sin\sigma \tag{24}$$

where

$$\sigma(deg) = a + 279.9348 + 1.914827 \sin a - 0.079525 \cos a + 0.019938 \sin 2a - 0.001620 \cos 2a \tag{25}$$

The angular fraction of a year, a, for a particular date is given by

$$a = 360(JO - 1)/365.242 \tag{26}$$

where JO = Julian date.

The solar hour angle, H, a measure of the longitudinal distance to the sun from the point for which the calculation is made, is given by

$$H(deg) = 15(ZO - M) - LO \tag{27}$$

where ZO = Greenwich mean time (GMT) of the calculation (hour);
M = Time of the meridian passage, or true solar noon (hour), and;
LO = Station longitude, positive being west of Greenwich (deg).

M is derived from

$$M = 12 + 0.12357 \sin a - 0.004289 \cos a + 0.153809 \sin 2a + 0.06078 \cos 2a \tag{28}$$

2.2.6 Calculating the stability parameter

Method 1 is based on a mathematical relationship of the Monin-Obukhov length, L, and surface roughness, Z_o, to the Pasquill stability categories. Golder (1972), by using data developed over five years, developed a nomogram relating the Monin-Obukhov length, L, (m) and surface roughness, Z_o, (m) to the Pasquill stability categories, a mathematical relationship between L, Z_o, and the stability parameter, SP. The following relationship was found:

$$SP = A + B\log_{10}(100Z_o) \quad (29)$$

where $A = 3.5 + 21.67/L$

$B = 0.48$ when $|1/L| > 0.015$; $= 43.63\,|1/L|^{1.08}$ when $|1/L| < 0.015$; $= -B$ when $1/L < 0$

Z_o and L are in m, and Z_o is restricted to the 0,001-0,40 m range in the model.

Values of *SP* are allowed to vary from 0.5 to 6.0. Extrapolating below 0.5 is not very reliable, and using 0.5 as the minimum value is a conservative approach. For *SP* value of 6, which happens at nighttime under light wind conditions, the model assumes that horizontal meandering occurs. When concentration averaging times are greater than 1 minute, the model assumes a stability parameter for horizontal diffusion of 3.5, or a neutral condition. Concentrations taken over averaging times of 1 minute or less are considered to be unaffected by the rather large oscillation period of the meandering wind. Since meandering does not affect vertical diffusion, the stability parameter of the vertical diffusion remains at 6. For an inversion based less than 50 m above the ground during day or night, the stability parameter is set at 6.0. At night, when meandering may be occurring, the SP for horizontal diffusion is set at 3.5 when the concentration averaging time is greater than 1 minute.

The approach of **method 2** is based on the Modified Sigma Theta (MST) by Mitchell (1982). If the standard deviation of the horizontal wind direction σ_θ is known. For nighttime, when σ_θ is greater than 12.5 degrees, Mitchell assumes that the large σ_θ is due to meandering and not instability. Since meandering does not affect vertical diffusion, an adjustment is made in the stability classes for vertical diffusion. The MST method is summarized in Table 3.

TABLE 3: Modified sigma theta (MST) method to determine atmospheric stability class (from Mitchell, 1982)

σ_θ (°)	**Daytime stability class[2]**	**Wind speed (ms^{-1})**	**Nighttime[1] stability class[3]**
$\sigma_\theta > 22.5$	A	$u < 2.4$	G
		$2.4 < u < 2.9$	F
		$2.9 < u < 3.6$	E
		$3.6 < u$	D
$22.5 > \sigma_\theta > 17.5$	B	$u < 2.4$	F
		$2.4 < u < 3.0$	E
		$3.0 < u$	D
$17.5 > \sigma_\theta > 12.5$	C	$u < 2.4$	E
		$2.4 < u$	D
$12.5 > \sigma_\theta > 7.5$	D	All windspeeds	D
$7.5 > \sigma_\theta > 3.8$	E	all windspeeds	E
$3.8 > \sigma_\theta > 2.1$	F	all windspeeds	F
$2.1 > \sigma_\theta$	G	all windspeeds	G

[1]Nighttime is defined as the period from 1 hour before sunset to 1 hour after sunrise.
[2]More applicable to describing horizontal dispersion parameter σ_y at night.
[3]More applicable to describing vertical dispersion parameter σ_z at night.

For averaging periods of 1 minute or less, concentrations are less affected by the rather large oscillation period of the meandering wind. Hence, the stability parameter for the horizontal diffusion is set to equal the more stable stability parameter for vertical diffusion.

Since σ_θ values in Table 3 are for a 10 m level and a 60 minute time period, measured σ_θ for a height other than 10 m and time period other than 1 hour, must be adjusted to a 10 m height and a 60 minute time period. This is done by adjusting the σ_θ to the 10 m height as follows:

$$(\sigma_\theta)_{10} = \sigma_\theta(10Z)^{-0.2} \tag{30}$$

then adjusting the 10 m σ_θ to the 60 minute time period using

$$(\sigma_\theta)_{60} = (\sigma_\theta)_{10}(60/t)^{0.2} \tag{31}$$

where Z is the wind measurement height and t is the time period over which σ_θ is measured.

The following equation in AFTOX is used for determining of all stability parameters (SP) in all cases except for the stability parameter for vertical dispersion at night when $\sigma_\theta > 12.5°$:

$$SP = 6.46 - 0.341\sigma_\theta + 0.0045\sigma_\theta^2 \tag{32}$$

where σ_θ is now the corrected σ_θ for a 10 m height and 60-minute period.

Determination of stability parameters by the model for nighttime when $\sigma_\theta > 12.5$ degrees is shown in Table 4.

TABLE 4: The nighttime stability parameter for vertical dispersion as a function of σ_θ and wind speed

σ_θ (degrees)	Wind speed (m/s)	Vertical stability parameter (SP)
$\sigma_\theta > 22.5$	$u > 4.1$	$SP = 3.5$
	$2.4 < u < 4.1$	$SP = 14.4/u$
	$u < 2.4$	$SP = 6.0$
$22.5 > \sigma_\theta > 17.5$	$u > 3.4$	$SP = 3.5$
	$2.0 < u < 3.4$	$SP = 12/u$
	$u < 2.0$	$SP = 6.0$
$17.5 > \sigma_\theta$	$u > 2.7$	$SP = 3.5$
	$1.9 < u < 2.7$	$SP = 9.6/u$
	$u < 1.9$	$SP = 5.0$

The AFTOX model makes three exceptions to the MST method:

1) During daytime, no matter how small the σ_θs are, the model does not allow, as in Method 1, the stability parameters to exceed 3.5 (D stability class). In other words, only unstable or neutral conditions exist during the daytime.

2) Anytime, day or night, that the height of the inversion base is less than 50 m above the ground, the stability parameter for vertical diffusion is adjusted to 6.0.

3) As in Method 1, during meandering wind or low inversion conditions, the stability parameter for

the horizontal diffusion is set equal to the more stable stability parameter for concentration averaging periods of 1 minute or less.

2.3 Estimation of plume rise

The plume height is used in the calculation of the vertical term. The Briggs plume rise equations are discussed below. The description follows Appendix B of the Addendum to the MPTER User's Guide (Chico and Catalano, 1986) for plumes unaffected by building wakes. The distance dependent momentum plume rise equations, as described in Bowers, et al. (1979) are used to determine if the plume is affected by the wake region for building downwash calculations. These plume rise calculations for wake determination are made assuming no stack-tip downwash for both the Huber-Snyder and the Schulman-Scire methods.

2.3.1 Stack-tip downwash

In order to consider stack-tip downwash, modification of the physical stack height, h_s, is performed following Briggs (1974). The modified physical stack height, h_s', is found from:

For $v_s < 1.5v$

$$h'_s = h_s + 2d_s[\frac{v_s}{u_s} - 1.5] \tag{33}$$

and for $v_s \geq 1.5$

$$h'_s = h_s$$

where h_s = Physical stack height (m);
v_s = Stack gas exit velocity (m/s), and;
d_s = Inside stack top diameter (m).

This h_s' is used throughout the remainder of the plume height computation. If stack tip downwash is not considered, $h_s' = h_s$ in the following equations.

2.3.2 Buoyancy and momentum fluxes

For most plume rise situations, the value of the Briggs buoyancy flux parameter, F_b (m^4/s^3), is needed.

$$F_b = gv_s d_s^2(\frac{\Delta T}{4T_s}) \tag{34}$$

where ΔT = $T_s - T_a$, T_s is stack gas temperature (K), and;
T_a = Ambient air temperature (K).

For determining plume rise due to the momentum of the plume, the momentum flux parameter, F_m (m^4/s^2), is calculated based on the following formula:

$$F_m = v_s^2 d_s^2 \frac{T_a}{4T_s} \tag{35}$$

2.3.4 Unstable- or neutral-crossover between momentum and buoyancy

For cases with stack gas temperature greater than or equal to ambient temperature, it must be determined whether the plume rise is dominated by momentum or buoyancy. The crossover temperature difference (ΔT_c), is determined by setting Briggs' (1969) Equation 5.2 equal to the combination of Briggs' (1972) Equations 6 and 7, and solving for ΔT, as follows:

For $F_b < 55$,

$$(\Delta T)_c = \frac{0.0297\, T_s v_s^{1/3}}{d_s^{2/3}} \tag{36}$$

and for $F_b \geq 55$,

$$(\Delta T)_c = 0.00575\, T_s \frac{v_s^{2/3}}{d_s^{1/3}} \tag{37}$$

If the difference between stack gas and ambient temperature, ΔT, exceeds or equals $(\Delta T)_c$, plume rise is assumed to be buoyancy dominated, otherwise plume rise is assumed to be momentum dominated.

2.3.5 Unstable- or neutral-buoyancy rise

For situations where ΔT exceeds $(\Delta T)_c$ as determined above, buoyancy is assumed to dominate. The final effective plume height, h_e (m), is determined from the equivalent of the combination of Equations 36 and 37 (Briggs, 1972):

For $F_b < 55$:

$$h_e = h'_s + 21.425 \frac{F_b^{3/4}}{u_s} \tag{38}$$

and for $F_b \geq 55$:

$$h_e = h'_s + 38.71 \frac{F_b^{3/5}}{u_s} \tag{39}$$

2.3.6 Unstable - or neutral-momentum rise

For situations where the stack gas temperature is less than or equal to the ambient air temperature, the assumption is made that the plume rise is dominated by momentum. If ΔT is less than $(\Delta T)_c$ from Equation 36 or 37, the assumption is also made that the plume rise is dominated by momentum. The plume height is calculated from Equation 40 (Briggs, 1969):

$$h_e = h'_s + 3 d_s \frac{v_s}{u_s} \tag{40}$$

Briggs (1969) suggests that this equation is most applicable when v_s/u_s is greater than 4.

3. METEOROLOGICAL PARAMETERS AND CHOICE OF SITES FOR METEOROLOGICAL INFORMATION

The meteorological parameters required by both models are surface observation data and the upper air observation data which are obtained by sending a sensor attached to a balloon into the atmosphere. The sensor sends signals to the computer at the surface. The model requires hourly surface data for temperature, dry bulb temperature, cloud cover, cloud height, wind speed and direction. Upper air data that is required is the mixing layer height. Isc3View can estimate the mixing layer heights from the hourly surface data.

Keflavík airport was chosen as the site for the meteorological information, that representative of the meteorological conditions at Svartsengi power plant. This was in view of the fact that at the airport, there is a regular hourly collection of surface observation data, and upper air data twice a day. It is located about 12 km from Svartsengi and the topography between these two areas is fairly flat. The wind speed and direction at Svartsengi can therefore be expected to be similar to that at the airport.

3.1 Wind patterns at Svartsengi

The meteorological information for Svartsengi was obtained from Keflavík Airport where a 24 hour meteorological weather station is run.

Wind analysis was done for the period between August 1994 to February 1995, representing the period that H_2S measurements were taken. Figure 2 shows the average wind patterns from August to December 1994. It is evident that the dominant wind patterns are northerly and northeasterly. This means that transport of H_2S is to the south and southwesterly sectors. Month to month wind roses are shown in Figures 3-7.

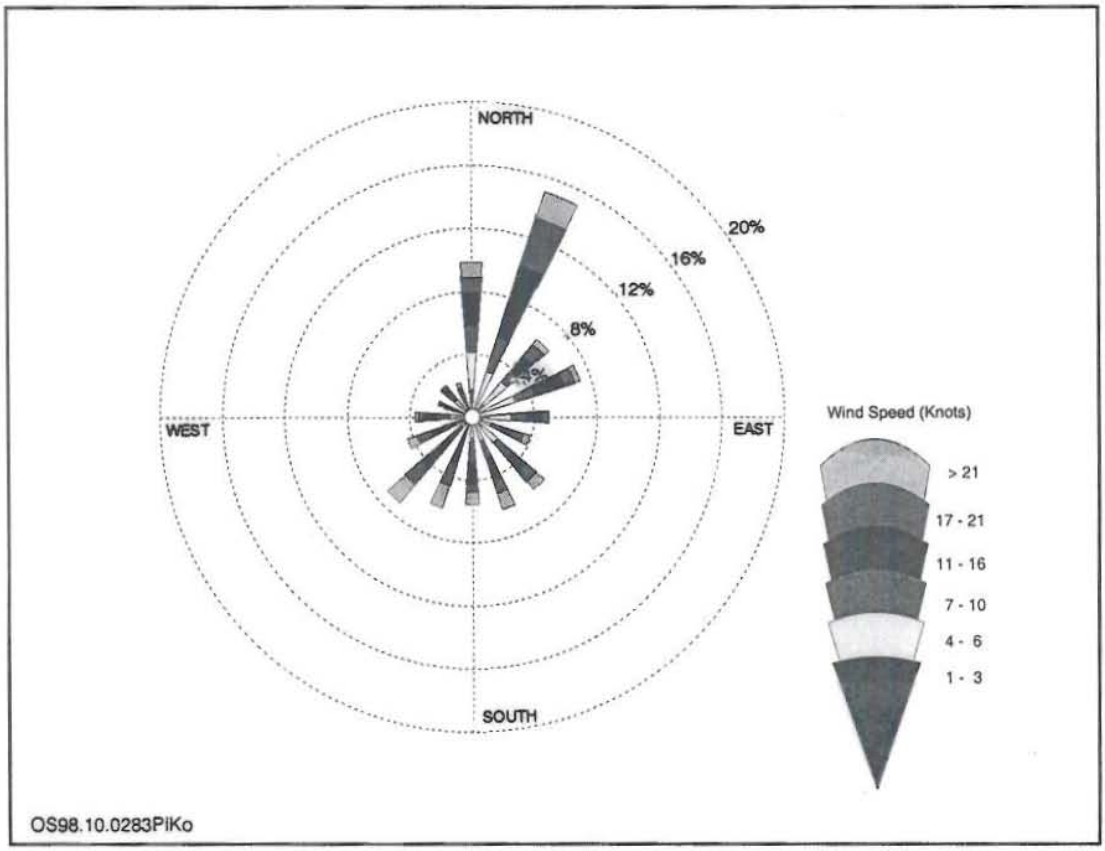

FIGURE 2: Wind rose plot for Keflavík, August 3rd - December 1994

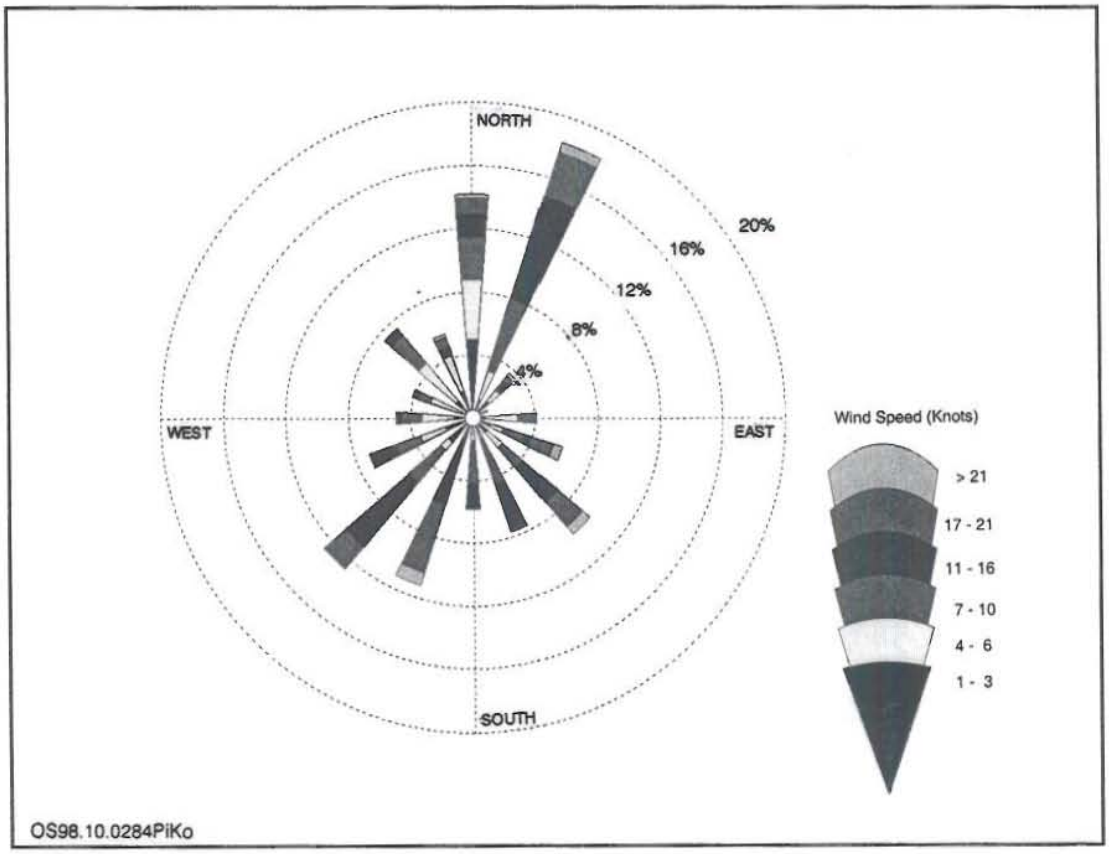

FIGURE 3: Wind rose plot for Keflavík, August 1994

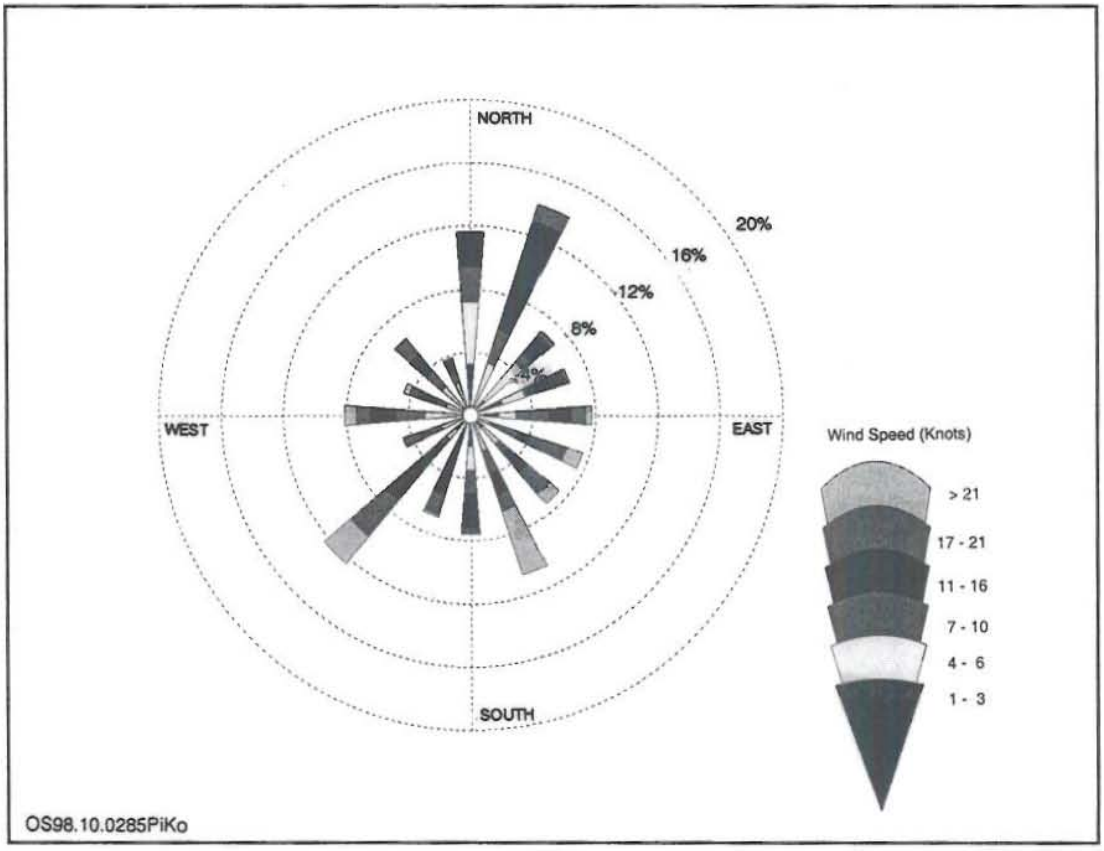

FIGURE 4: Wind rose plot for Keflavík, September 1994

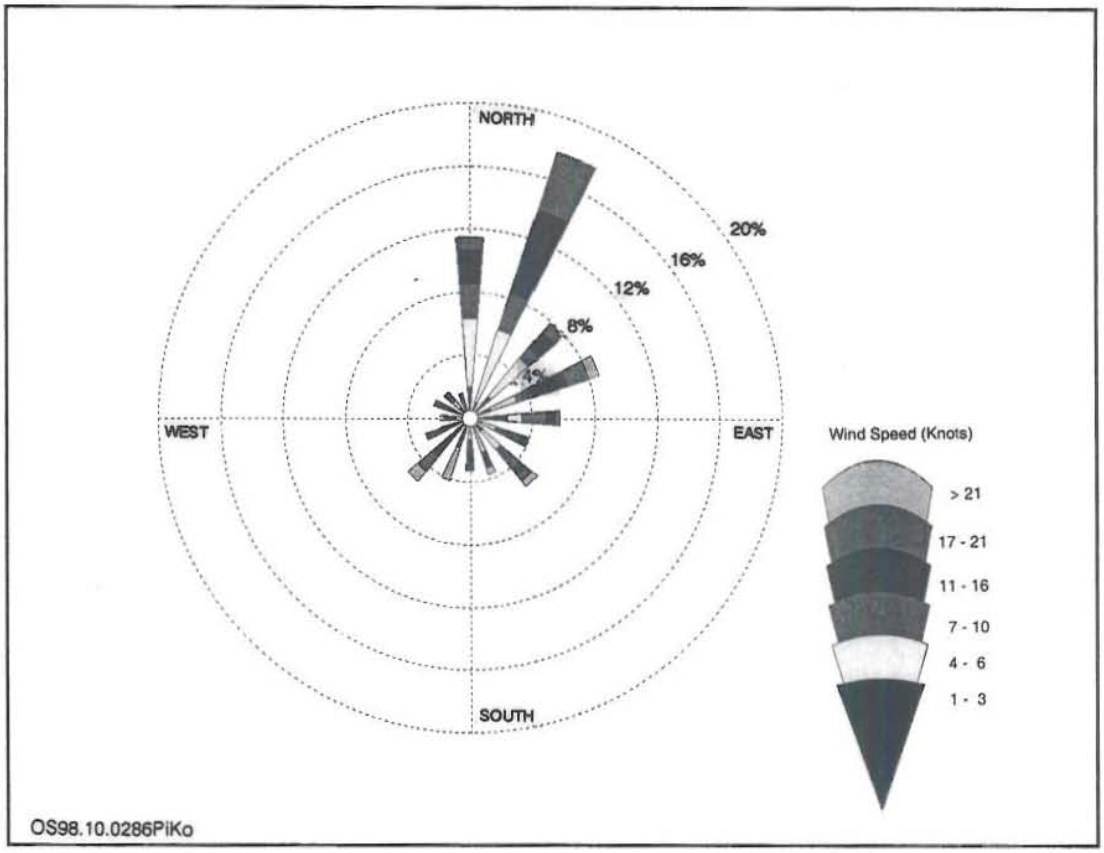

FIGURE 5: Wind rose plot for Keflavík, October 1994

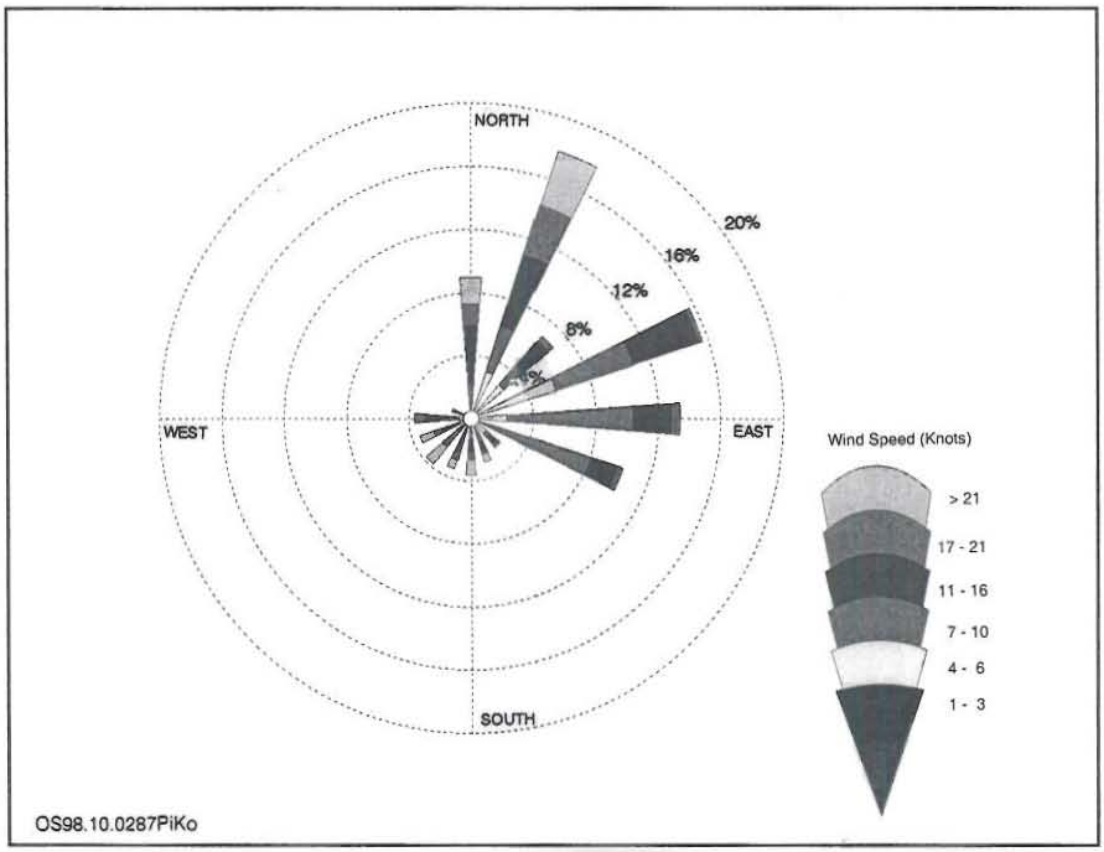

FIGURE 6: Wind rose plot for Keflavík, November 1994

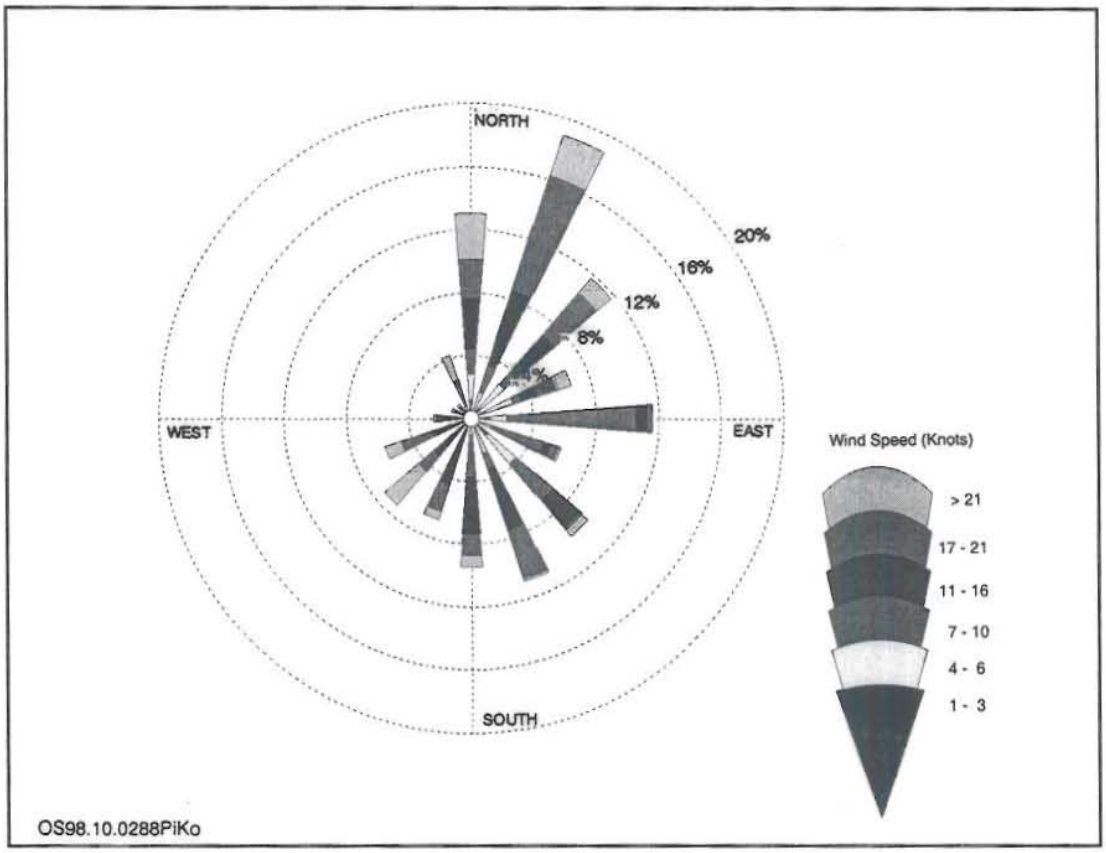

FIGURE 7: Wind rose plot for Keflavík, December 1994

In August, the winds are quite variable, but mainly north-northeasterly and south-southwesterly. During this period the most frequent wind speeds are in the range 7-10 knots. In September, just like August, winds are variable, a northerly wind is dominant with southwest-southerly winds prevailing. Wind speeds are in the range of 11-16 knots. The month of October is generally characterised by north-northeasterly flow patterns, with relatively low wind speeds, 4-6 knots. In November, the flow is mainly north-northeasterly, while December exhibits some variable winds, north-northeasterly and south-southeasterly. In January, the main flow is easterly, with wind speeds of the range 7-10 knots dominating.

3.2 Missing data

Since the model uses hourly observation data, in cases where there is no data for a given hour, the average of the two readings one before the hour with missing information, and the other after the missing hour data, is taken. For the case where there are three hourly observations like cloud height and cover, data for hours without observations were taken as those nearest to the observed hour.

3.3 H_2S collection and measurement method

The H_2S collection for the Svartsengi power plant was done under the auspices of the Hitaveita Reykjavikur company and National Energy Authority, Orkustofnun. In the study carried out in 1994, long term measurements were done over a period of about 6 months, from August 1994 to February 1995. During this time the sampling collection period was over 24 hours.

3.3.1 24 hour collection

Whatman 40 paper filters are soaked in 0.5 ml of 2% Ag_2NO_3 solution, put on glass filters (Whatman GF/D), and dried under vacuum overnight. After that, they are put in the filter holders. During collection H_2S is bound to silver as silver sulphide (Ag_2S). Leftover silver, all silver that does not bind to H_2S is rinsed out from the filters with 10 ml of 0.1 M NaCN solution for approximately 2 hours. Silver sulphide is then dissolved with nitric acid (conc. HNO_3) in a hot sand bath. The silver is then analysed in an Atomic Absorption Spectrophotometer. Silver (Ag) is recalculated as µg H_2S. The comparison filters are treated in the same way as the collection filters. Air sampling was done by using a sampler, where a given volume of air was collected over the 24 hour duration.

3.3.2 Short term measurements

The short term measurements were performed by using the Jerome 621 sampler. A pump draws air into the flow system and through a scrubber. The sample bypass opens, shunting unfiltered sample air onto the gold film H_2S sensor. The sensor absorbs and integrates the hydrogen sulphide from the sample, the sample bypass closes, and the additional filtered air passes over the sensor sweeping any sample carry-over from the sensor chamber. The measured concentration of H_2S is displayed, in ppb, on the metre. This value remains displayed on the metre until the next sample is initiated. The in-situ measurements were taken by averaging the five measurements taken at 14 s puff. Therefore, the average readings can be taken to be representative of 1 minute H_2S concentration.

4. MEASURED CONCENTRATIONS AND RESULTS FROM METEOROLOGICAL MODELLING

4.1 Statistical analysis of the H_2S analysis at Svartsengi

Daily H_2S data for the Svartsengi area, collected over the period August - December 1994, were analysed for percentiles. First the data for the whole collection period was analysed, then monthly analytical data. Results of the analysis for the mean values, 50th and 90th percentiles are shown in Table 6. The same results are expressed on a histogram (Figure 8).

TABLE 6: H_2S concentrations (µg/m^3) at Svartsengi power plant

Period	August-December	August 1994	September 1994	October 1994	November 1994	December 1994	January 1995
50th percentiles	10.4	6.27	10.81	11.39	10.4	13.14	9.67
90th percentiles	15.38	11.94	15.83	15.24	13.56	16.34	15.52
Maximum	20.63	13.3	18.07	17.37	16.42	20.25	20.63

It can be noted from the above results that generally there is an increasing trend in H_2S concentrations from August, where lower values were recorded, to maximum values in December. There is very little variation in monthly concentrations.

Results of point measurements carried out under the auspices of Orkustofnun and Hitaveita Reykjavíkur (Ívarsson et al.,1993) on August 10th 1993, found concentrations in the range of 0-265 µg/m^3. However, this was done on just a single day, and at each point, sampling was done for a very short time. This, therefore, does not reflect the expected average H_2S concentrations.

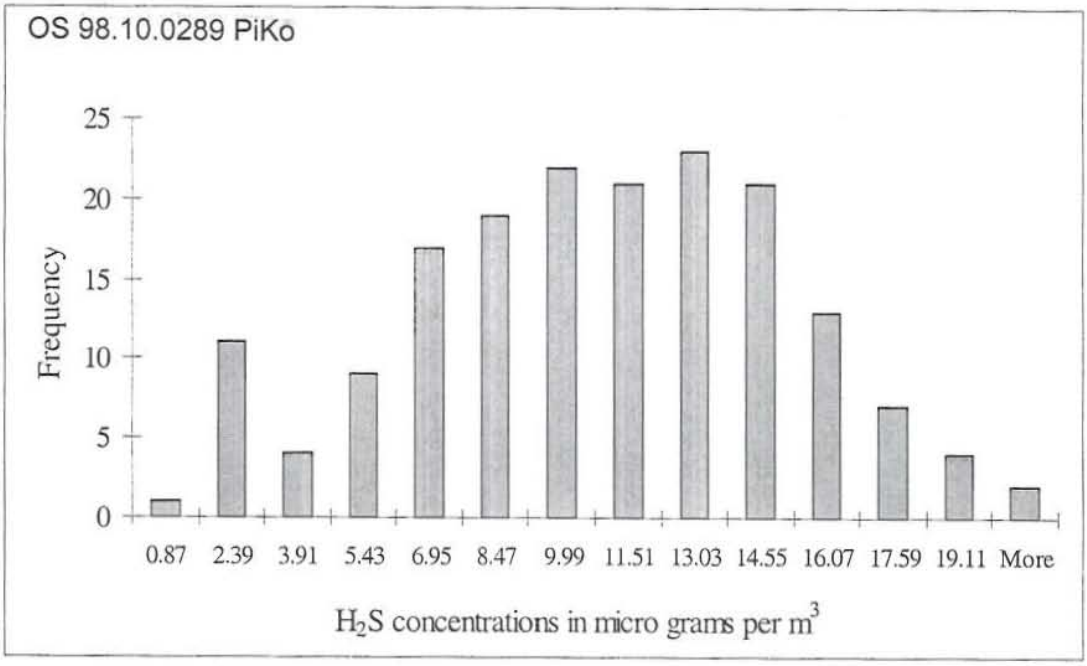

FIGURE 8: H_2S histogram for Svartsengi power plant

4.2 Isc3View predictions

The model was used to predict 1, 3, 8 and 24 hourly H_2S concentrations. Monthly and 5 month concentrations were also considered. In the Isc3View model, the following emission parameters were used:

(i)	Stack height	18 m;
(ii)	Stack exit diameter	0.5 m;
(iii)	Stack exit temperature	368 K;
(iv)	Gas exit velocity	5 m/s;
(v)	H_2S flow rate	10.75 g/s.

Results for short term predictions are shown in Figures 9-14, showing the model simulations at different averaging times. From Figure 9, it is evident that 1 hour average concentrations do not occur evenly distributed around the power station. The maximum concentration is located further away from the power station, almost 200 m. The model simulates maximum concentrations of 1720 $\mu g/m^3$. The northeastern and the southern sectors of the power plant show higher concentrations than the other sectors. This can be explained by the 5 month wind rose plots which clearly show dominant northerly and southerly winds. Higher concentrations are, therefore, expected to be in these zones.

Concentrations over a 3 hour averaging period depict a similar pattern, whereby high concentrations occur in the southern and northern sectors. It is also clear that the highest concentration is not at the power plant, but about 200 m away. This is because the source is at an elevated site, 18 m in this case, and the plume rises, before touching the ground at a distance from the source. The maximum concentration is 1190 $\mu g/m^3$.

Concentrations averaged over an 8 hour period are similar in the distribution pattern, but the maximum concentration is much smaller (680 $\mu g/m^3$). The model predicts higher daily averages (maxima 264 $\mu g/m^3$) than were observed during the measurement period, between August 1994 - February 1995.

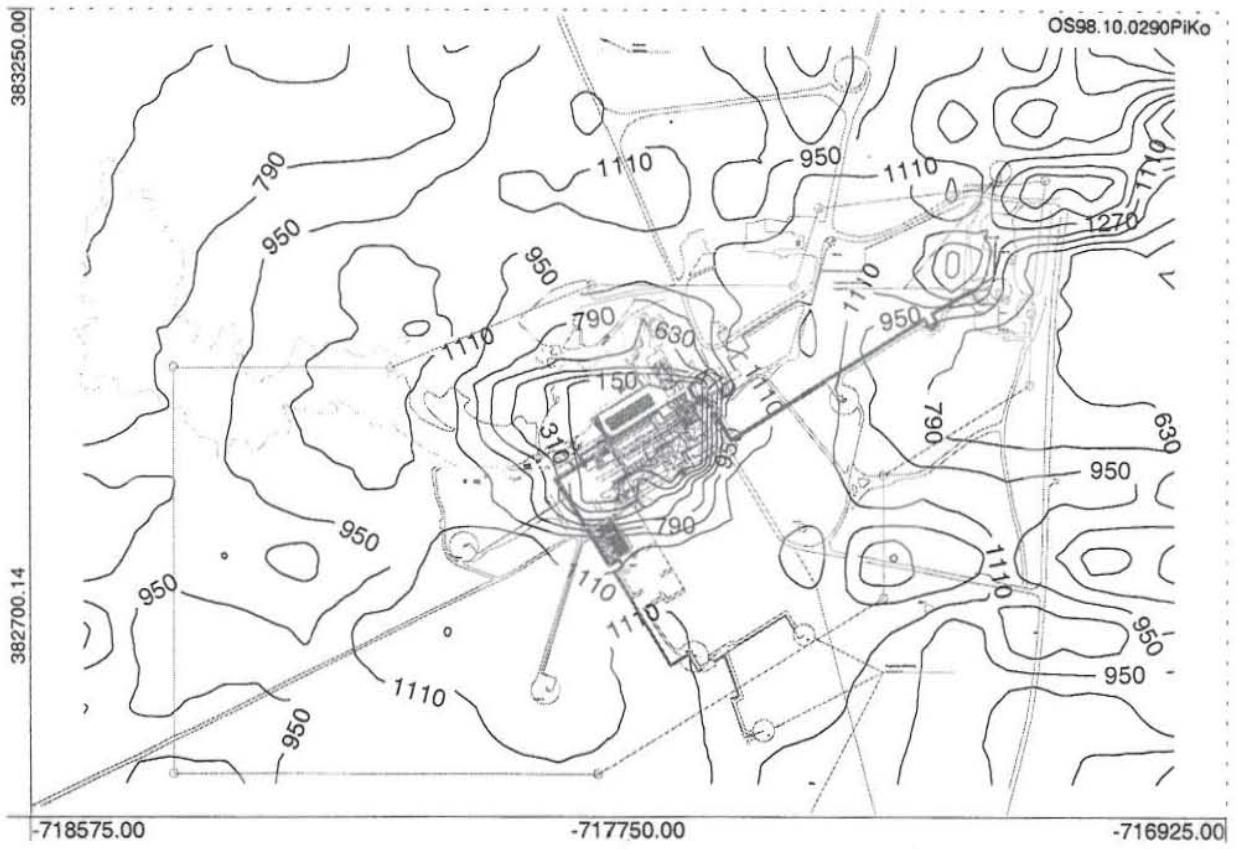

FIGURE 9: Average 1 hour hydrogen sulphide concentration (µg/m^3) at Svartsengi power plant

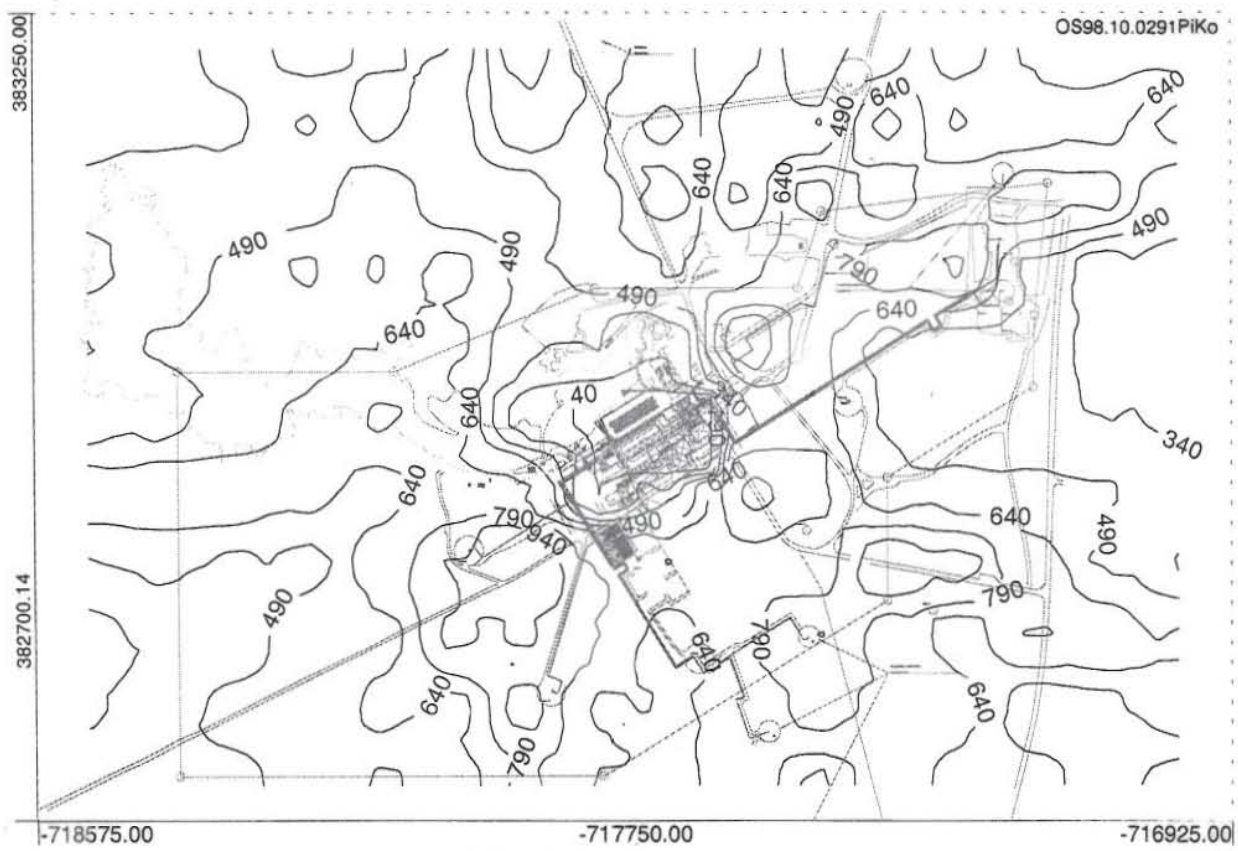

FIGURE 10: Average 3 hour hydrogen sulphide concentration (µg/m^3) at Svartsengi power plant

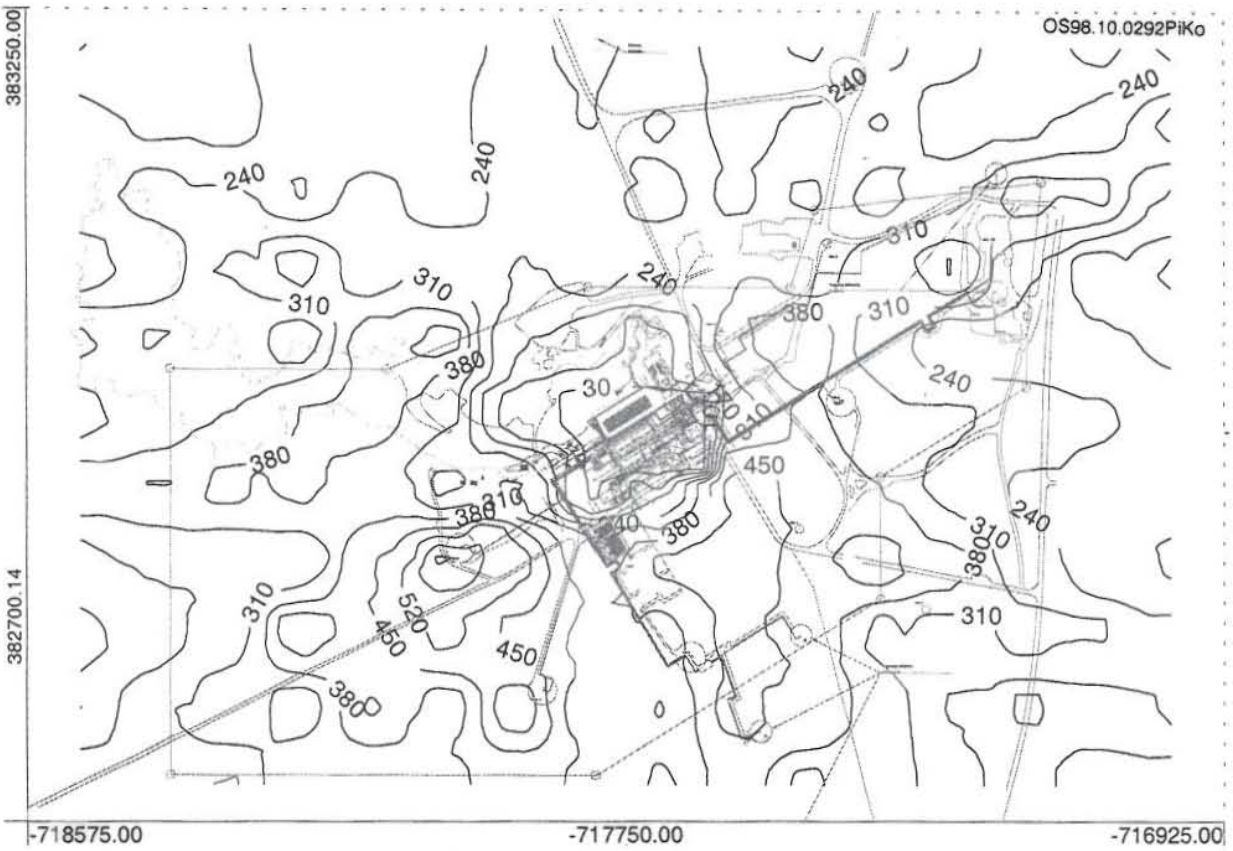

FIGURE 11: Average 8 hour hydrogen sulphide concentration (µg/m³) at Svartsengi power plant

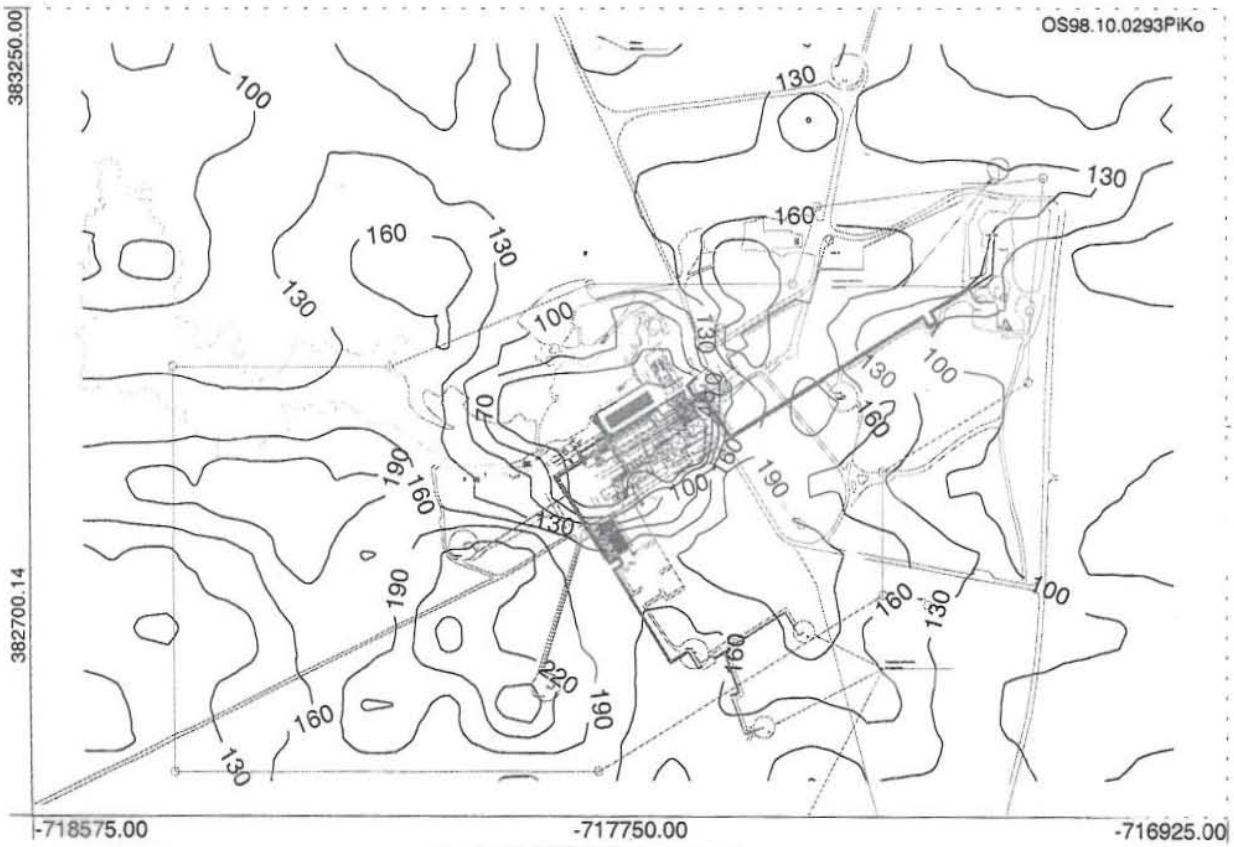

FIGURE 12: Average 24 hour hydrogen sulphide concentration (µg/m³) at Svartsengi power plant

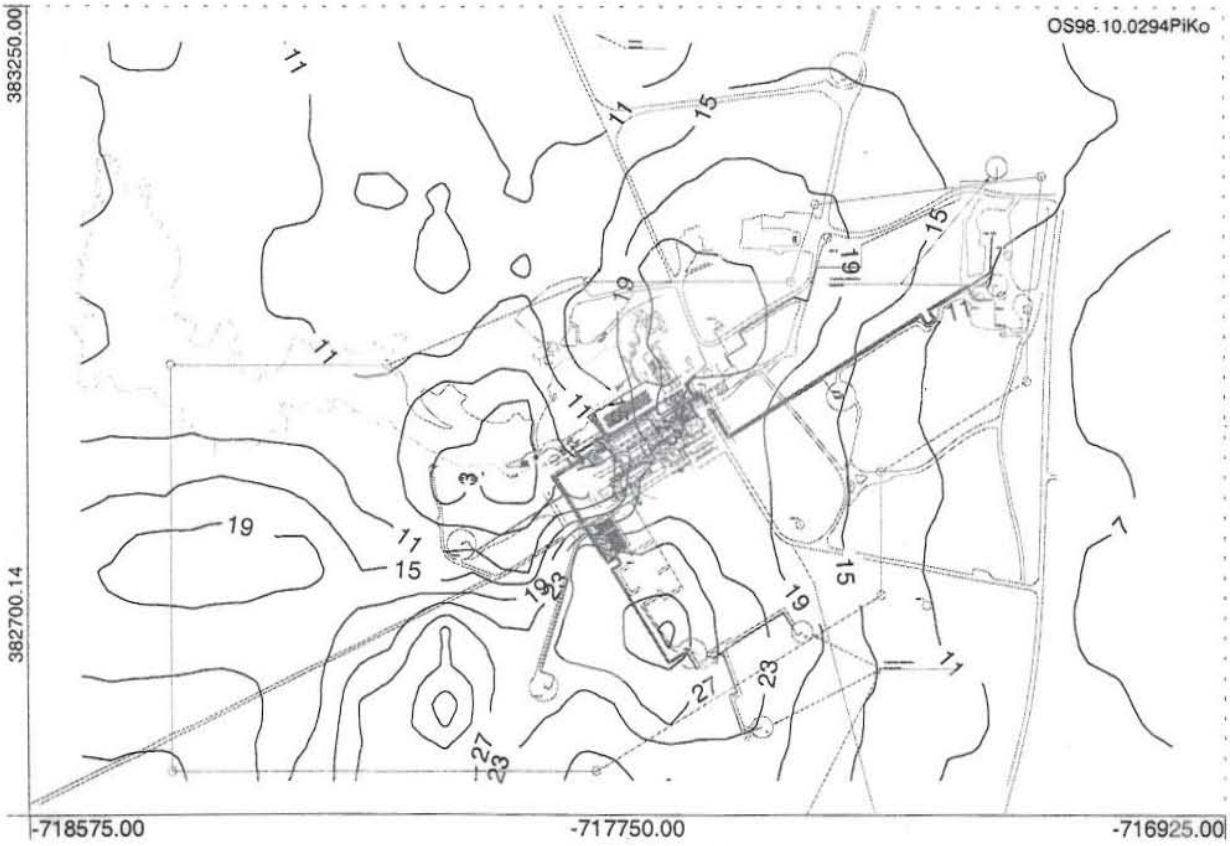

FIGURE 13: Average monthly hydrogen sulphide concentration (μg/m^3) at Svartsengi power plant

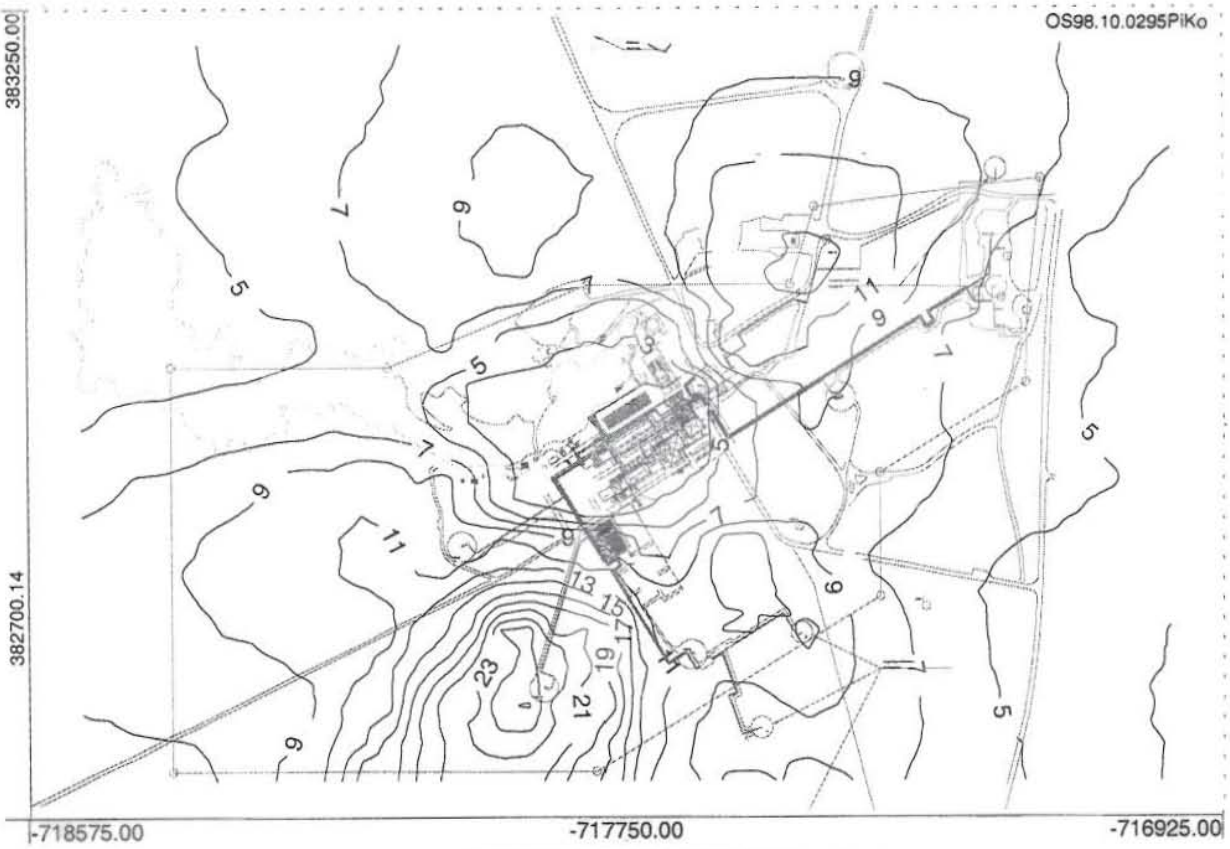

FIGURE 14: Average hydrogen sulphide concentration (μg/m^3) for August-December 1994 at Svartsengi power plant

During this period, the maximum daily concentration was about 20 $\mu g/m^3$. However it should be noted that the instrument for the collection of air for H_2S analysis at Svartsengi for 24 hour periods, was always closer to the power plant building. The siting, therefore, could hardly allow for recording of maximum probable concentrations. Location of the equipment was such that it gets a constant power supply. The building has the effect of generally blocking the flow. Turbulent wakes also generated by the building can lead to high groundlevel concentrations a few metres from the building in the down-wind direction.

The monthly and 5 month average concentrations are considerably smaller than the short term averages. The maximum concentration over a 5 month period was 28 $\mu g/m^3$. This compares well to the 90th percentile value (15 $\mu g/m^3$), measured over the same period.

4.3 The AFTOX model

This was used to predict short term concentrations of 1 minute, 1 hour and 24 hour concentrations. Since this model does not use continuous meteorological conditions over the averaging time, average meteorological conditions were used. The following meteorological conditions are assumed:

(i) Stability class D;
(ii) Surface atmospheric pressure 1004 mbar;
(iii) Average temperature of 5°C;
(iv) Average wind speed of 4 knots;
(v) Wind direction of 225 degrees.

These conditions were assumed to be average conditions expected in July-August. This was the time when short term sampling was done under the auspices of Hitaveita Reykjavíkur and Orkustofnun. In determining short term averages, the roughness length was chosen to be 0.03 m (this describes terrain of runway, open flat terrain, grass, and a few isolated obstacles, AFTOX 4.0, 1991). Results for 1 minute predictions, assuming different emission scenarios and roughness lengths, are shown in Figures 15-17.

The maximum concentrations for 1 minute averaging times are similar for both cases, reaching a maximum of 1400 $\mu g/m^3$ for the worst case scenario, stability class F, roughness length, 0.03

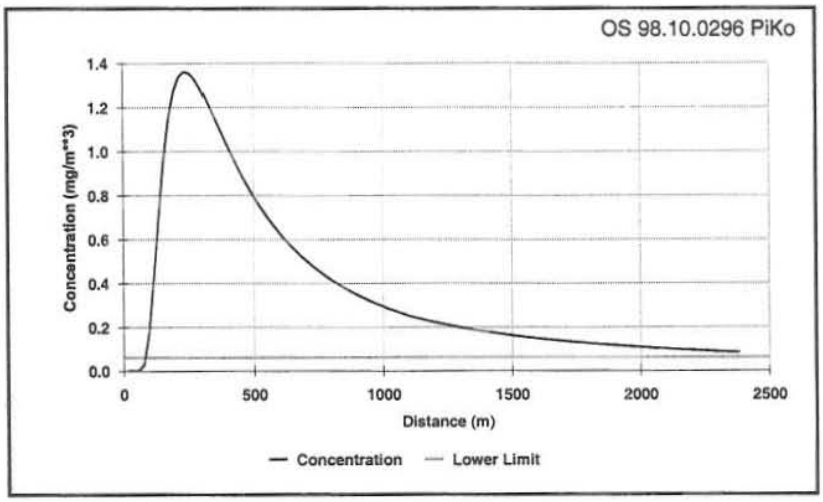

FIGURE 15: One minute H_2S centre line concentration at Svartsengi, stability class F and roughness length, 0.03 m

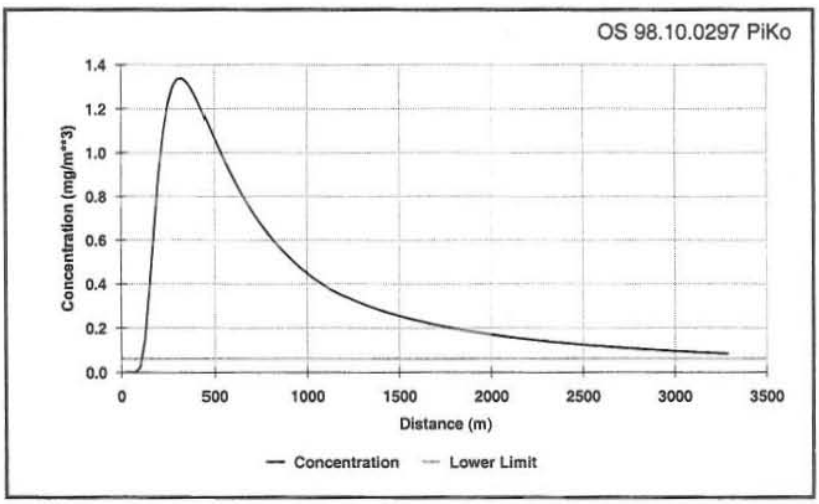

FIGURE 16: One minute H_2S centre line concentration at Svartsengi, stability class D and roughness length, 0.03 m

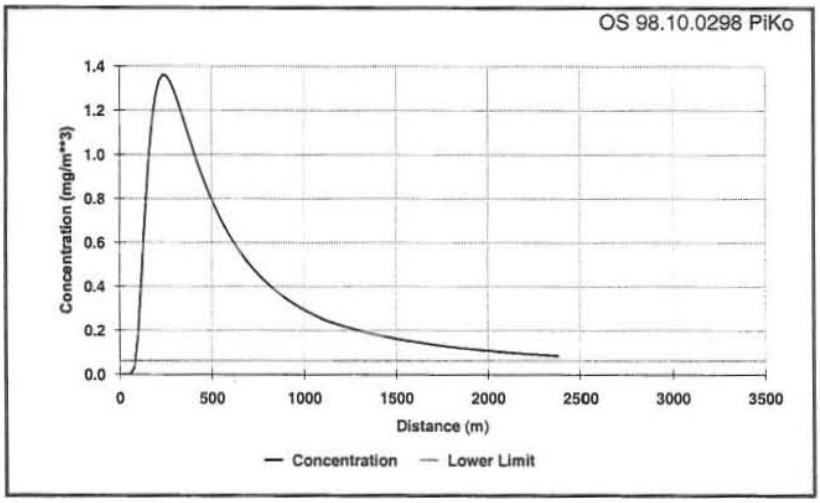

FIGURE 17: One minute H_2S centre line concentration at Svartsengi, stability class D and roughness length, 0.1 m

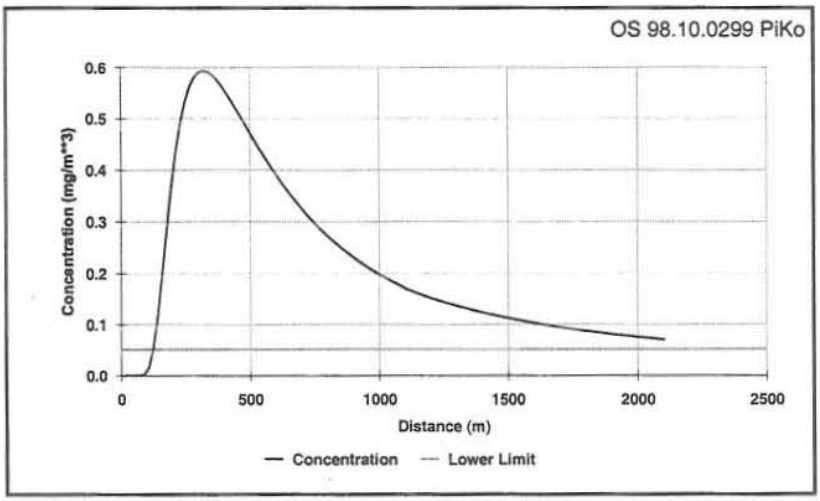

FIGURE 18: One hour H_2S centre line concentration at Svartsengi, stability class D and roughness length, 0.03 m

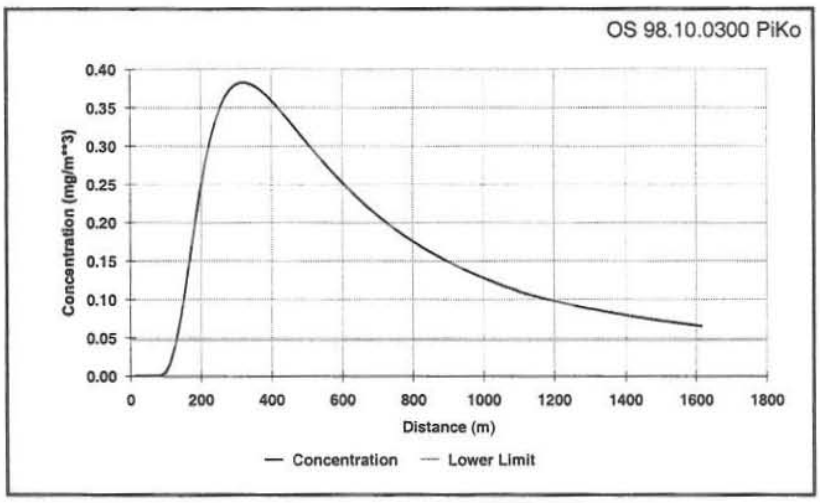

FIGURE 19: 3 hour H_2S centre line concentration at Svartsengi, stability class D and roughness length, 0.03 m

m (Figure 15). While using the same roughness length, but assuming stability class D, roughness length, 0.03 m, the results follow a similar pattern (Figure 16), but the peak concentration is slightly lower (1330 $\mu g/m^3$). Figure 17 shows the case for stability class D, and roughness length, 0.01 m. In this scenario, the maximum concentration attained is 1290 $\mu g/m^3$. For the case of lower roughness length, higher downwind concentrations are experienced than when using higher roughness length. The overall effect of increasing the roughness length is to retard the horizontal buoyancy-induced spreading of the plume and to enhance the mixing between plume and the environment. For low ground sources, increasing the roughness length will significantly reduce the concentrations. For the case of Svartsengi, however, a release height of 18 m is the point at which the gas is vented to the atmosphere. This height does not seem to have a large impact on the groundlevel concentrations down wind.

Hourly averages (Figure18), showed a similar pattern, with maximum (590 $\mu g/m^3$) occurring about 180 m down wind. Concentrations then decrease at almost an exponential rate as one moves away from the source.

A similar concentration pattern is shown on a 3 hour average curve (Figure19), with maxima of 380 $\mu g/m^3$ occurring and similar results we see for the 8 hour average (Figure 20). In the Isc3View model, the maximum 1-hour concentration was 1200

$\mu g/m^3$. This shows an underestimation by a factor of about two. Concentrations decline as the averaging time increases just like the case of the Isc3View model. The AFTOX model predicts maximum concentrations of 310 $\mu g/m^3$ for a 24 hour averaging time (Figure 21), which compares quite well with results obtained while using the Isc3View model 280 $\mu g/m^3$.

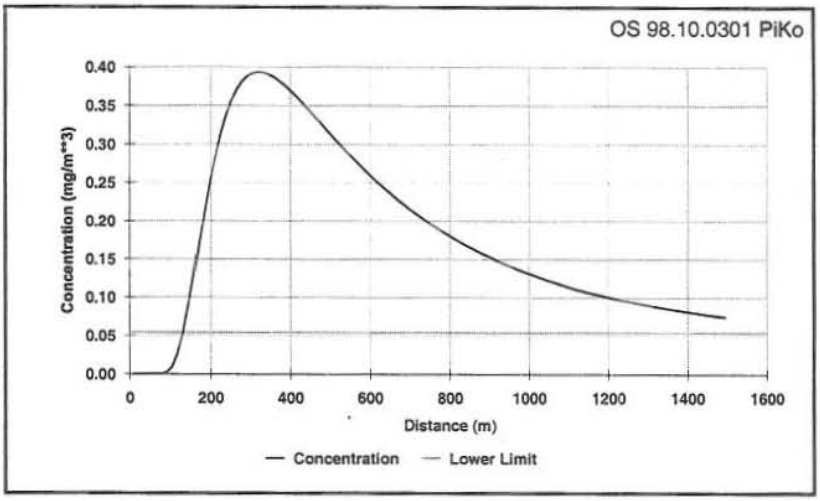

FIGURE 20: 8 hour H_2S centre line concentration at Svartsengi, stability class D and roughness length, 0.03 m

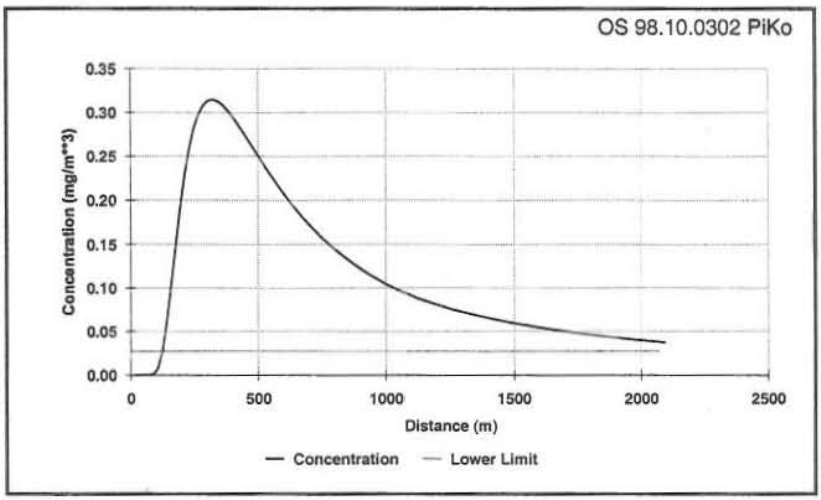

FIGURE 21: 24 hour H_2S centre line concentration at Svartsengi, stability class D and roughness length, 0.03 m

5. SUMMARY AND CONCLUSIONS

Based on the results obtained from the two models and the data obtained during the sampling period, the following conclusions and recommendations can be made.

(i) Both the Isc3View and AFTOX models predict maximum concentrations away from the source point;
(ii) Long term H_2S measurements at Svartsengi are in agreement with the Isc3View model results, but the model gives higher predictions for the short term averaging period;
(iii) The Isc3View model gives more representative results;
(iv) Svartsengi is generally characterised by high wind speeds, thus diluting the H_2S from the plume.

In order to predict H_2S at Svartsengi with more precision, I would like to make the following recommendations;

(i) Long term monitoring of H_2S should be done at Svartsengi to give average concentrations; a continuous data log could be more useful than a 24-hour sampler, since it would give concentrations averaged over a longer time, and would, therefore, smooth out the peak concentrations;
(ii) There is need to have representative sampling points generally away from obstacles that hinder smooth air flow;
(iii) Future work studies should include larger areas;
(iv) There is a need to ascertain the representativeness of Keflavík meteorological data to the Svartsengi area.

ACKNOWLEDGEMENTS

Special thanks to the UNU and the government of Iceland for funding this course and to Dr. Ingvar Fridleifsson and Lúdvík S. Georgsson for the organisation of this work. I would like to sincerely thank my supervisor Hreinn Hjartarson for meteorological data acquisition, interpretation and critically reading my report. I am also grateful to Halldór Ármannsson for co-ordinating the environment course, as well as Hrefna Kristmannsdóttir and Sverrir Thórhallsson. The assistance from Hitaveita Reykjavíkur is highly appreciated. I will not forget Gudrún Bjarnadóttir for her support during my stay, Gudrún Jónsdóttir and Skúli Víkingsson for their efforts in organising for me the Svartsengi topographical map, and to the other lecturers and the entire staff of Orkustofnun. I am greatly indebted to Mark Hilverda of Lakes Environment for his technical assistance with ISC3View model through Internet. Finally I would like to express my gratitude to Kenya Electricity Generating Company (KenGen) for granting me a sabbatical leave in order to attend the six months course.

REFERENCES

AFTOX 4.0., 1991: *The Air Force toxic chemical dispersion model - a user's guide.* Trinity Consultants Inc., Environmental Research Papers, No. 1083, 62 pp.

Bowers, J.F., Bjorklund, J.R., and Cheney, C.S., 1979: *Industrial source complex (ISC) dispersion model user's guide.* U.S. Environmental Protection Agency, North Carolina, report EPA-450/4-79-030, Vol. I, 275 pp.

Briggs, G.A., 1969: *Plume rise.* National Technical Information Service, Springfield, Virginia, USAEC Critical Review Series, TID-25075, 81 pp.

Briggs, G.A., 1972: Discussion on chimney plumes in neutral and stable surroundings. *Atmos. Environ., 6,* 507-510.

Briggs, G.A., 1974: *Diffusion estimation for small emissions.* U.S. Atomic Energy Commission, Oak Ridge, Tennessee, report ATDL-106.

Chico, T., and J.A., Catalano, 1986: *Addendum to the user's guide for MPTER.* U.S. Environmental Protection Agency, North Carolina, Contract No. EPA 68-02-4106, 85 pp.

Cox, R.A., and Sandalls, F.J., 1974: The photo-oxidation of hydrogen sulphide and dimethyl sulphide in air. *Atmos Environment. 8,* 1269-1281.

Cox, R.A., and Shepherd D. 1980: Reactions of OH radicals with gaseous sulphur compounds. *Nature, 20*, 330-331.

DeBruin, H.A.R., and Holtslag, A.A.M., 1982: A simple parameterization of the surface fluxes of sensible and latent heat during daytime compared with the Penman-Monteith concept. *J. Appl. Meteorol, 21*, 1610-1621.

Golder, D., 1972: Relations between stability parameters in the surface layer. *Boundary Layer Met. 3*, 46-58.

Holtslag, A.A.M., and Van Ulden, A.P., 1983: A simple scheme for day time estimates of the surface fluxes for routine weather data. *J. Climate Appl. Meteorol. 22*, 517-529.

Ívarsson, G., Sigurgeirsson, M.A., Gunnlaugsson, E., Sigurdsson, K.H., Kristmannsdóttir, H., 1993: *Measurement of gas in atmospheric air*. Orkustofnun and Hitaveita Reykjavíkur, Reykjavík, report OS-93074/JHD-10 (in Icelandic), 69 pp.

Kasten, F, and Czeplak, G, 1980: Solar and terrestrial radiation dependent on the amount and type of cloud. *Solar Energy, 24,* 177-189.

Mitchell, A.E. Jr., 1982: A comparison of short term dispersion estimates resulting from various atmospheric stability classification methods. *Atmos. Environ. 16*, 765-773.

Ragland, K.W., and Dennis, B.L., 1975: Point source atmospheric diffusion model with variable wind and diffusivity profiles. *Atmos. Environ, 9*, 175-189.

Salerno, R. and Clerici G,C., 1995: Transport and dispersion from cooling towers in the complex topography of the Tuscany geothermal areas. *Proceedings of the World Geothermal Congress 1995, Florence, Italy, 4*, 2747-2751.

Sinclair Knight, and ESA Pty Ltd., 1994: *Environmental assessment.* KPC, North East Olkaria Power development Project, draft report.

Smith, F.B., 1972: A scheme for estimating the vertical dispersion of a plume from a source ground level. *Proceedings of the Third Meeting of the Expert Panel on Air Pollution Modelling, NATO committee on the Challenges of Modern Society, Paris, France.*

US Environmental Protection Agency 1995: *User's guide for industrial source complex (ISC3) dispersion models.* US Environmental Protection Agency, report EPA-454/B-95-003b.

Woolf, H.M., 1980: *On the computation of solar elevation angles and the determination of sunrise and sunset times.* National Meteorological Centre, Environmental Sciences Services Administration, Hillcrest Heights, MO.